Lattice dynamics of $KTa_{1-x}Nb_xO_3$ solid solutions in the cubic phase

G. E. Kugel and M. D. Fontana
Centre Lorrain d'Optique et d'Electronique du Solide, Technopole de Metz, 2 rue Edouard Belin, F-57045 Metz Cédex 03, France

W. Kress
Max-Planck-Institut für Festkörperforschung, Heisenbergstrasse 1, D-7000 Stuttgart 80, Federal Republic of Germany
(Received 19 May 1986)

We have calculated the phonon dispersion curves of mixed crystals of $KTaO_3$ and $KNbO_3$ for various niobium concentrations. In our calculations, a nonlinear shell model is used, in which the fourth-order anharmonic core-shell interaction of the oxygen ions is taken into account in the self-consistent phonon approximation. The measured phonon dispersion curves, their temperature dependence, and, in particular, the temperature dependence of the ferroelectric soft-mode frequency for different niobium concentrations between 0 and 100 at. % are well reproduced by our calculations in which only two coupling parameters depend on the niobium concentration in a systematic way. These two parameters are temperature independent and characterize the linear and nonlinear polarizability of the oxygen ions. All other coupling parameters are temperature and concentration independent.

I. INTRODUCTION

The solid solution $KTa_{1-x}Nb_xO_3$ (KTN) is an interesting system for the investigation of ferroelectric phase transitions and the understanding of their nature. It has a rather complex phase diagram and allows a systematic investigation of the dynamical properties of a system in which the fundamental microscopic parameters can be varied continuously by changing the niobium concentration x. The temperature dependence of the frequency and the damping of the ferroelectric or incipient ferroelectric soft mode, the transition temperature T_c and the character of the phase transitions depend strongly on the niobium concentration x.[1-3] In order to illustrate the phase diagram we first consider the two limiting cases of the system.

$KNbO_3$ and $KTaO_3$ behave quite differently. $KNbO_3$ is a proper ferroelectric.[4] It undergoes a sequence of three phase transitions. With decreasing temperature it transforms from the high-temperature cubic phase first at 703 K to the tetragonal phase, then at 490 K to the orthorhombic phase, and finally at 210 K to the low-temperature rhombohedral phase. Close to the cubic-to-tetragonal phase transition a strong increase of the static dielectric constant is observed.[5] This increase in the dielectric constant can only partly be explained by the softening of the ferroelectric mode as deduced from the far-infrared reflectivity spectra.[6,7] In both the cubic and the tetragonal phase the values of the static dielectric constant calculated by the Lyddane-Sachs-Teller relation from the measured optic-phonon frequencies derived from the reflectivity spectra[6,7] are much lower than those observed in direct measurements. The ferroelectric soft mode is strongly overdamped in both the cubic and the tetragonal phase and becomes underdamped in the vicinity of the orthorhombic to rhombohedral phase transition. It turns out that the nature of the phase transitions in $KNbO_3$ is rather complicated. A crossover from a displacive to an order-disorder mechanism near T_c has been proposed.[6]

The other limiting case is $KTaO_3$. Pure $KTaO_3$ is an incipient ferroelectric which behaves like a ferroelectric in its paraelectric phase but does not undergo any phase transition. It shows a strong increase of the dielectric constant ϵ_0 with decreasing temperature. The increase of ϵ_0 is related to the softening of the ferroelectric mode which has been studied intensively by infrared, Raman, and neutron spectroscopy.[8-12] Moreover, the soft mode of $KTaO_3$ has been investigated recently by hyper-Raman scattering.[13] This technique yields directly the frequency and damping of the ferroelectric soft mode with better accuracy than other methods.

The properties of $KTaO_3$ are drastically modified when small amounts of niobium are added. Above potassium niobate concentrations of 0.8 mol % KTN becomes ferroelectric at low temperatures. The transition temperature increases with increasing niobium concentration. This is due to the strengthening of the dipolar interactions in a system with competing dipolar fluctuations and long-range ordering forces. Dielectric susceptibility and acoustic measurements in KTN have revealed various crossovers from displacive to other regimes.[1-3,14,15] The temperature dependence of the soft mode has been investigated recently by hyper-Raman measurements of $KTa_{1-x}Nb_xO_3$ for niobium concentrations x of 0.008, 0.012, and 0.020.[16] The results of these experiments show clearly deviations from the classical Curie-Weiss law. For temperatures down to 30 K above T_c a mean-field law with a critical exponent $\gamma=1$ is found for the dielectric susceptibility. At lower temperatures the critical behavior depends strongly on the niobium concentration. For $x=0.008$ a quantum regime with a critical exponent $\gamma=2$ is found.[17] The measurements for $x=0.012$ yield a mode-coupling behavior with $\gamma=1.4$. For higher concen-

trations a strong damping prevents the observation of deviations from the Curie-Weiss law close to the phase transition.

A large amount of various experimental data has been accumulated in recent years concerning the temperature dependence of the ferroelectric soft mode in KTN in a wide range of temperatures (20—1300 K) and niobium concentrations (Refs. 1, 6, 13, 16, 18, and 19). The aim of this paper is to give a theoretical interpretation of this data and to point out the relevant physical interactions which govern the dynamical properties and lead to the ferroelectric phase transition. For this purpose we use a shell model in which the anharmonic fourth-order on-site interactions in the core-shell coupling describe the softening of the ferroelectric mode. Since we are primarily interested in the temperature and concentration dependence of the frequency of the ferroelectric mode, we have completely neglected the third- and fourth-order intersite interactions, which cause small temperature shifts of the other modes. The third-order terms, which vanish because of symmetry reasons for the on-site interactions, provide essential contributions to the linewidth, although the strong damping of the ferroelectric mode for high niobium concentrations is still an open problem which can not be solved by taking into account third-order intersite couplings only. However, our simplified treatment of the anharmonic terms provides a clear insight in the driving mechanism for the softening of the ferroelectric mode.

II. MODEL DESCRIPTION

A. Anharmonic lattice models

Ferroelectric phase transitions are due to a critical cancellation of the long-range dipolar forces and the short-range overlap forces.[20–22] In the harmonic approximation one of the polar modes, the ferroelectric soft mode, is unstable. Above the phase transition, this mode is stabilized by anharmonic contributions.[22–24] A mean-field treatment of the anharmonic contributions leads to a Curie-Weiss law for the temperature dependence of the soft-mode frequency:

$$\omega_f^2 = a(T - T_c)^\gamma , \tag{1}$$

where $\gamma = 1$ is the critical exponent.

Various microscopic models have been used for the driving mechanism of the phase transition.[25–27] In these models the harmonic phonon frequencies are renormalized by anharmonic contributions to the self-energy. One of the most complete treatment has been given by Bruce and Cowley[26] for $SrTiO_3$. These authors include thermal strain and cubic and quartic Ti-O and Sr-O couplings but do not consider the anharmonic on-site core-shell coupling of the oxygen ions. Their model yields good agreement with various available experimental data but does not give a clear insight into the driving mechanism for the softening of the ferroelectric mode. Since in this paper we focus on the softening of the ferroelectric mode, we consider a simplified model which includes in its anharmonic part only the quartic on-site interactions of the oxygen ions. Indeed, a careful inspection of ferroelectric materials shows that more than 90% of them contain either oxygen or other chalcogen ions. Furthermore, these compounds exhibit strong second-order Raman spectra. For the rocksalt structure crystals (MgO,SrO), it has been shown[28,29] that the second-order Raman spectra of these compounds are mainly due to intra-ionic polarizabilities of the oxygen ion. This suggests that intra-ionic polarizabilities of the O^{-2} ion are also the driving mechanism for the softening for the ferroelectric mode in oxidic perovskites. Thus, Migoni *et al.*[30,31] introduced a fourth-order on-site core-shell interaction of the oxygen ion in the classical shell model. The self-consistent phonon solutions of the equations of motion of this model reproduce the temperature dependence of the soft mode at $q = 0$ as well as the two-phonon Raman spectra of $KTaO_3$ and $SrTiO_3$. Simplified versions of this model[32,33] have been applied to ferroelectric perovskites[34] and to other ferroelectric materials.[35–37] These simplified models are based on quasi-one-dimensional diatomic chains of polarizable anionic clusters (TiO_6 or TaO_6 octahedrons) and rigid cations. In the harmonic case, the soft-mode instability can be attributed to a negative core-shell coupling constant g_2 of the cluster, which involves the oxygen polarizability as well as the attractive Coulomb forces. The stabilization by anharmonicity is due to the intra-ionic fourth-order coupling parameter g_4 of the cluster which describes the nonlinear on-site core-shell contribution.

B. The three-dimensional polarizability model

In our calculations we have used the three-dimensional anharmonic shell model of Migoni *et al.*[30] In this model, the anisotropy of the oxygen polarizability is described by two different linear coupling constants $k_2^{\text{O-K}}$ (in the direction of the K ions) and $k_2^{\text{O-}B}$ (in the direction of the Ta or Nb ions). The nonlinear fourth-order contribution is taken into account by a coupling constant $k_4^{\text{O-}B}$ which acts only in the direction of the ion B. The contribution $k_4^{\text{O-K}}$ which acts in the direction of the K ion is considered small and has been neglected.

The core-shell on-site potential ϕ can be expanded in terms of relative shell displacements $\mathbf{w}$ as

$$\phi^{\text{O-K}} = \tfrac{1}{2} k_2^{\text{O-K}} \sum_{l,\alpha,\beta} w_\beta^2 \begin{bmatrix} l \\ \text{O}_\alpha \end{bmatrix}, \quad \alpha \neq \beta \tag{2}$$

and

$$\phi^{\text{O-}B} = \tfrac{1}{2} k_2^{\text{O-}B} \sum_{l,\alpha} w_\alpha^2 \begin{bmatrix} l \\ \text{O}_\alpha \end{bmatrix} + \frac{1}{4!} k_4^{\text{O-}B} \sum_{l,\alpha} w_\alpha^4 \begin{bmatrix} l \\ \text{O}_\alpha \end{bmatrix}, \tag{3}$$

where α and β label Cartesian components, l is the cell index, and O_α indicates the oxygen ion located on the line O—B which connects oxygen and transition metal in the α direction.

The nonlinear term leads in the self-consistent phonon approximation to a temperature-dependent core-shell coupling constant $k_{\text{O-}B}(T)$ which acts in the O-B direction and is given by

$$k_{\text{O-}B}(T) = k_2^{\text{O-}B} + \tfrac{1}{2} k_4^{\text{O-}B} \langle w_{\text{O-}B}^2 \rangle_T . \tag{4}$$

The thermal average $\langle w_{\text{O-}B}^2 \rangle_T$ of the relative displace-

ment in the O-B direction can be written as

$$\langle w^2_{\text{O-}B}\rangle_T=\frac{\hbar}{2NM_0}\sum_{\mathbf{q},j}\frac{f^2_\alpha\left[\mathrm{O}_\alpha,\begin{matrix}\mathbf{q}\\ j\end{matrix}\right]}{\omega(\mathbf{q},j)}\coth\left[\frac{\hbar\omega(\mathbf{q},j)}{2\kappa_B T}\right], \quad (5)$$

where M_0 is the mass of the oxygen ion, N is the number of $\mathbf{q}$ points considered in the summation, κ_B is the Bolzmann constant, and $\omega(\mathbf{q},j)$ is the frequency of the phonon with branch index j and wave vector $\mathbf{q}$. The shell eigenvectors $\mathbf{f}\binom{\mathbf{q}}{j}$ are given by

$$\mathbf{f}\begin{bmatrix}\mathbf{q}\\ j\end{bmatrix}=-\underline{M}^{-1/2}(\underline{\tilde{S}})^{-1}\underline{T}^{\dagger}\underline{M}^{-1/2}\mathbf{e}\begin{bmatrix}\mathbf{q}\\ j\end{bmatrix}, \quad (6)$$

where $\underline{M}$ is the diagonal matrix of the masses and $\underline{T}$ and $\underline{\tilde{S}}$ are the core-shell and shell-shell coupling matrices, respectively. These coupling matrices contain both short-range and Coulomb interactions. Note that in this paper "shells" always refers to the relative displacements $\mathbf{w}$ of the shells. The eigenvectors of the dynamical matrix $\underline{D}$ [see Eq. (9)] are denoted by $\mathbf{e}\binom{\mathbf{q}}{j}$. The shell-shell interaction matrix $\underline{\tilde{S}}$ contains in our case diagonal parts $\underline{K}_2$ and $\underline{\Delta}$ which arises from the harmonic and anharmonic core-shell coupling, respectively:

$$\underline{\tilde{S}}=\underline{S}+\underline{K}_2+\underline{\Delta}, \quad (7)$$

where $\underline{S}+\underline{K}_2$ is the usual harmonic contribution and

$$\Delta^{\kappa\kappa'}_{\alpha\beta}=\tfrac{1}{2}k^{\text{O-}B}_4\langle w^2_{\text{O-}B}\rangle_T\delta_{\alpha\beta}\delta_{\kappa\mathrm{O}_\alpha}\delta_{\kappa'\mathrm{O}_\alpha} \quad (8)$$

is the additional contribution which is due to the nonlinear coupling in the mean-field approximation. The nonlinear part of the polarizability renormalizes the dynamical matrix:

$$\underline{D}=\underline{M}^{-1/2}[\underline{R}-\underline{T}(\underline{S}+\underline{K}_2+\underline{\Delta})^{-1}\underline{T}^{\dagger}]\underline{M}^{-1/2}, \quad (9)$$

where $\underline{R}$, $\underline{T}$ and $\underline{S}$, are the Fourier transforms of the force-constant matrices in customary notation; they include the corresponding Coulomb interactions.

The harmonic shell model is specified by 15 parameters.[38–40] The six short-range parameters $A_{\text{K-O}}$, $B_{\text{K-O}}$, $A_{B\text{-O}}$, $B_{B\text{-O}}$, $A_{\text{O-O}}$, and $B_{\text{O-O}}$ are the axially symmetric force constants A and B between K-O, B-O, and O-O, respectively. The ionic and shell charges are given by Z_{K}, Z_B, Y_{K}, and Y_{O}. The parameters k_{K} and k_B are the core-shell interaction for the K and B ions (B stands for the group-VB atoms Ta and Nb). The core-shell interactions of the oxygen ion are specified by the coupling constants $k^{\text{O-K}}_2$, $k^{\text{O-}B}_2$, and $k^{\text{O-}B}_4$, already mentioned before.

C. Method of calculation

The harmonic shell model parameters on which our calculations are based are those obtained by Migoni *et al.*[41] by a new fit to a complete set of experimental dispersion curves in the three high-symmetry directions of $KTaO_3$. Shell model calculations with these parameters, which are listed in Table I, reproduce the measured phonon dispersion curves of $KTaO_3$ within experimental error.

A systematic comparison of recent measurements (Table II) shows that only little variation in phonon frequencies is observed when niobium is introduced in $KTaO_3$, except for the soft mode. These small changes are due to the changed masses and lattice constants. This finding is reinforced by recent hyper-Raman measurements on the KTN crystals which reveal that the TO_4 optic mode at 540 cm^{-1} remains nearly constant in frequency and in damping with increasing Nb concentration.[16] Consequently, it seems reasonable to assume that all model parameters for the whole KTN series, except the core-shell coupling constants, do not depend on the niobium concentration and that the differences in the soft-mode behavior are exclusively due to variations of the harmonic as well as the anharmonic part of the intra-ionic core-shell coupling constants. It is well known that the oxygen ion O^{2-} is instable as a free ion. In a crystal it is stabilized by the Coulomb field and by the hybridizations of the oxygen $2p^6$ orbitals with the d electrons of the neighboring Ta and Nb ions. The variation of niobium concentration leads to a modification of the boundary conditions, which essentially affects the on-site polarizability of the oxygen ion in the direction of the B ion (Ta or Nb). In our calculations the variation of the oxygen polarizability is taken into account by the concentration dependence of the two coupling constants $k^{\text{O-}B}_2$ and $k^{\text{O-}B}_4$ (see below). Using these parameters the temperature dependence of $k_{\text{O-}B}(T)$ is obtained self-consistently according to Eq. (4). The coupling constants $k^{\text{O-}B}_2$ and $k^{\text{O-}B}_4$ are treated as effective parameters averaged over the whole lattice. Of course, the change in mass and in lattice parameter is included in the calculation.

The numerical values of the linear and quartic expansion coefficients $k^{\text{O-}B}_2$ and $k^{\text{O-}B}_4$ have been calculated by using the following procedure. For each niobium concentration x, the function $k_{\text{O-}B}(T)$ is determined from the

TABLE I. Concentration-independent parameters of the model for KTN. These parameters have been obtained by Migoni *et al.* (Ref. 41) by a least-squares fit to the measured dispersion curves of $KTaO_3$. The concentration-dependent parameters $k^{\text{O-}B}_2$ and $k^{\text{O-}B}_4$ are given in Fig. 4.

Short-range interactions ($e^2/2v$ units)					
$A_{\text{K-O}}$	$B_{\text{K-O}}$	$A_{B\text{-O}}$	$B_{B\text{-O}}$	$A_{\text{O-O}}$	$B_{\text{O-O}}$
14.65	−1.01	359.0	−68.0	3.22	1.085

Ionic and shell charges (e units)					Core-shell coupling (e^2/v units)		
Z_{K}	Z_B	Y_{K}	Y_B	Y_{O}	k_{K}	k_B	$k^{\text{O-K}}_2$
0.82	4.84	−0.419	7.83	−3.01	1000.0	1283.0	410.0

TABLE II. Measured phonon frequencies at $q=0$ for various niobium concentrations x.

		Phonon frequencies (cm^{-1})								
		F_{1u}		F_{1u}		F_{2u} (silent)		F_{1u}		
x	T (K)	TO_1	LO_1	TO_2	LO_2	TO_3	LO_3	TO_4	LO_4	Ref.
0%	300 K	81	185	199	279	279	422	546	826	13
	300 K	85.1	188	199			425	549	833	8
			196							
	300 K	85		198				556		12
	300 K	88	184	199			421	547	838	9,10
1.8%	300 K	86	185	200			425	545	826	1
	1000 K	125	187	207			425	536	820	1
10%	300 K		188	202		282	422	554	830	19
36%	253 K	85	188	199			423	549	833	19
100%	730 K	100	191	199			419	520	821	
	910 K	116	192	201			418	516	820	6,7
	1180 K	136	193.5	203.5			418	512	815	

measured soft-mode frequency. Using these values of $k_{O\text{-}B}(T)$, the phonon frequencies $\omega(\vec{q}_j)$, the core eigenvectors $\mathbf{e}(\vec{q}_j)$ and the shell eigenvectors $\mathbf{f}(\vec{q}_j)$ are recalculated in the quasiharmonic approximation. In the next step, the thermal average of the oxygen shell displacements in the B ion direction $\langle w^2_{O\text{-}B}\rangle_T$ is determined [Eq. (5)]. Then we obtain the temperature-independent parameters $k_2^{O\text{-}B}$ and $k_4^{O\text{-}B}$ of the oxygen polarizability in the direction of the Ta or Nb ions by a linear least-squares fit to the function $k_{O\text{-}B}(T)$. The values obtained for $k_2^{O\text{-}B}$ and $k_4^{O\text{-}B}$ are reintroduced in the dynamical matrix [Eqs. (8) and (9)] and the procedure is continued until self-consistency is obtained.

III. RESULTS OF THE CALCULATIONS

A. Soft-mode behavior of the KTN system

Our calculations are essentially based on the temperature dependence of the ferroelectric soft-mode frequency. We have, however, also calculated the phonon dispersion curves in the whole Brillouin zone as a function of niobium concentration and of temperature. Our results compare favorably with the available experimental data. Two typical examples are reported in Sec. III C.

Figure 1 shows the experimental data of the ferroelectric soft mode and the results of our calculations. The data between 0 and 300 K are hyper-Raman results obtained by Vogt and Uwe[13] for pure $KTaO_3$ and by Kugel *et al.*[16] for $KTa_{1-x}Nb_xO_3$ ($x=0.008$, 0.012, and 0.020). The mean-field behavior extends down to about 30 K above the transition temperature T_c. Below this limit, deviations from the Curie-Weiss law have been detected. On the other hand, the Curie-Weiss regime extends to high temperatures. This has been observed recently by ir reflectivity measurements on $KNbO_3$ in the cubic phase by Fontana *et al.*[6] and on KTN with niobium concentration $x=0.018$ by Rytz *et al.*[19] The temperature dependence of the soft mode between 300 and 1300 K obtained by ir spectroscopy is shown in the inset of Fig. 1.

Only the mean-field region has been considered in our calculations. Thus we excluded both the points in the vicinity of T_c, where quantum, mode-coupling, or order-disorder deviations may occur, and the point at very high temperatures, which may be influenced substantially by higher-order anharmonic effects. The results of our calculations, presented as continuous lines in Fig. 1, show that the temperature dependence of the soft mode of KTN is adequately described by the model in a wide range of temperatures for niobium concentrations x ranging from 0 to 1.

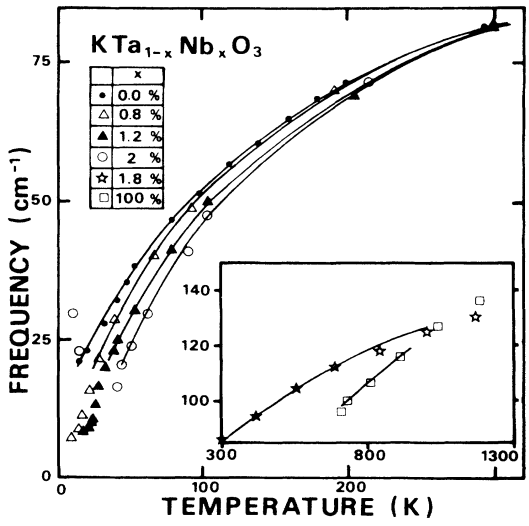

FIG. 1. Ferroelectric soft-mode frequency in the $KTa_{1-x}Nb_xO_3$ system as a function of temperature. The data between 0 and 300 K are hyper-Raman results (Refs. 13 and 16); those between 300 and 1300 K are ir reflectivity results (Refs. 6 and 18).

B. Analysis of the results

1. Temperature and concentration dependence of the polarizability

The frequency of the ferroelectric soft mode for a given temperature and for a given niobium concentration is determined by the oxygen-ion core-shell interaction $k_{O\text{-}B}(T)$. The temperature dependence of $k_{O\text{-}B}(T)$ is due to the thermal average as can be seen from Eqs. (4) and (5). Figure 2 represents the variations of $k_{O\text{-}B}(T)$ as a function of T for various x values. For a given temperature, the more important result is the decrease of $k_{O\text{-}B}(T)$ with increasing niobium concentration. This fact is particularly obvious in the inset of Fig. 2, where we report the results for KTN (1.8%) and for $KNbO_3$. The single point in the inset represents the neutron scattering result of Yelon *et al.*[42] for a KTN with $x=0.37$. It still fits into the scheme. These features mean that the polarizability of the O^{2-} ion in the direction of the B ions increases when going from $KTaO_3$ to $KNbO_3$. This is consistent with the increase of the transition temperature T_c with increasing niobium concentration.

2. Temperature and concentration dependence of the thermal average of the oxygen shell displacement $\langle w^2_{O\text{-}B}\rangle_T$

The increase of the polarizability in the direction of the B ion with increasing niobium concentration leads to an enhancement of the amplitude of the oxygen shell displacement $\mathbf{f}(^{q}_{j})$ and in consequence of the thermal average $\langle w^2_{O\text{-}B}\rangle_T$. Figure 3 shows the temperature and concentration dependence of the shell displacement vector

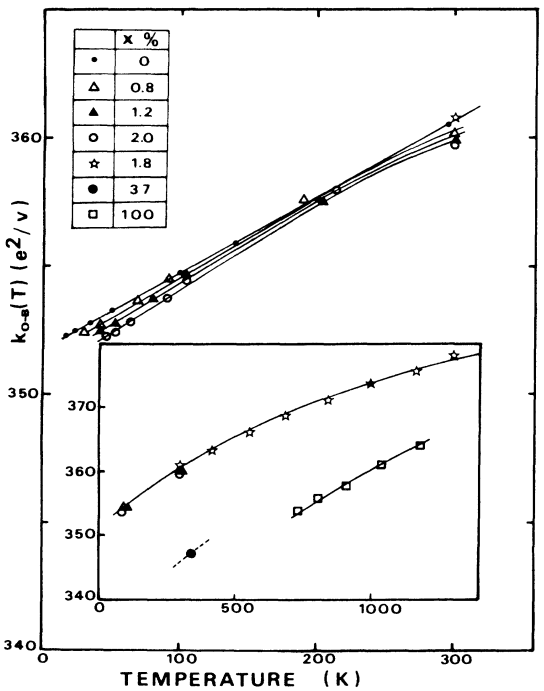

FIG. 2. Variation of the core-shell coupling constant $k_{O\text{-}B}(T)$ in the $KTa_{1-x}Nb_xO_3$ system as a function of temperature.

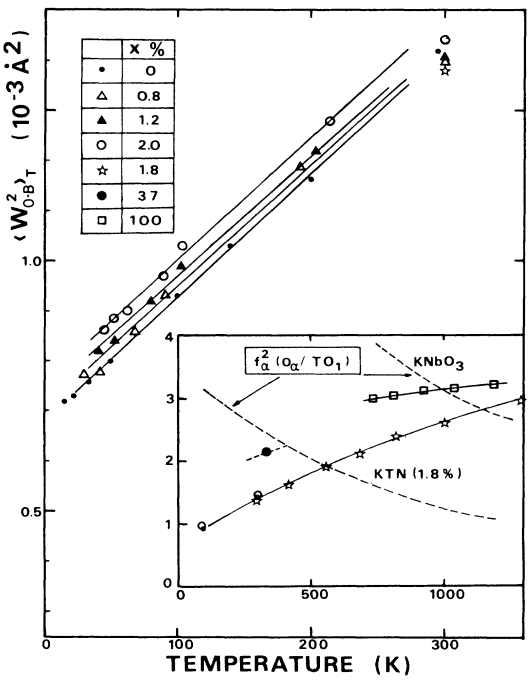

FIG. 3. Concentration and temperature dependence of the thermal average of the oxygen shell displacements $\langle w^2_{O\text{-}B}\rangle_T$ in the $KTa_{1-x}Nb_xO_3$ system. The amplitude squared of the oxygen shell displacements for two Nb concentrations (100% and 1.8%) is shown in the inset.

$\mathbf{f}_\alpha(O_\alpha,TO_1)$ and the thermal average of the shell displacement $\langle w^2_{O\text{-}B}\rangle_T$. The linear behavior of $\langle w^2_{O\text{-}B}\rangle_T$ is due essentially to the $\coth(\hbar\omega/k_BT)$ in Eq. (5). A systematic niobium concentration dependence of $\langle w^2_{O\text{-}B}\rangle_T$ at a given temperature is not easy to establish, since the experimental data for different concentrations, which are used in the fitting procedure, do not belong to the same temperature range. The comparison of the results for $x=0.012$ and $x=0.020$ obtained by hyper-Raman measurements[16] between 20 and 300 K with those obtained for $x=0.018$ from ir spectroscopy between 300 and 1300 K (Ref. 19) shows the coherence of the experimental data in two distinct temperature ranges and insures the reliability of the calculations with varying niobium concentrations. Moreover, the thermal average calculated from the neutron scattering data for $x=0.37$ (Ref. 42) fits in a satisfactory way in the general scheme. Another interesting feature revealed by our calculations (c.f. inset of Fig. 3) is the strong enhancement of the shell eigenvectors $\mathbf{f}_\alpha(O_\alpha,^{q}_{j})$ when temperature approaches the Curie temperature. This result clearly indicates that the driving mechanism of the phase transition is strongly related to the anisotropic and nonlinear deformabilities of the oxygen charge density along the O-B chains.

3. Concentration dependence of the core-shell coupling constants $k_2^{O\text{-}B}$ and $k_4^{O\text{-}B}$

The concentration dependence of the coupling parameters $k_4^{O\text{-}B}$ and $k_2^{O\text{-}B}$ is shown in Fig. 4. The linear constant

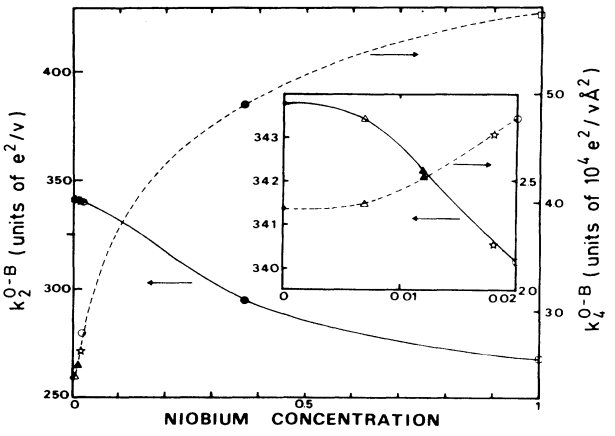

FIG. 4. Concentration dependence of the coupling parameters k_2^{O-B} and k_4^{O-B}.

k_2^{O-B} decreases slightly from about $340e^2/v$ to $270e^2/v$. The nonlinear parameter k_4^{O-B} shows a completely different behavior and increases drastically from about $2.4\times10^4 e^2/v\text{Å}$ to $5.6\times10^4 e^2/v\text{Å}$. v means the volume of the elementary cell. This reflects the fact that the oxygen polarizability increases with increasing niobium concentration and that the nonlinearity is consequently enhanced. The outer $2p^6$ electrons of the oxygen ion are strongly delocalized along the O-Nb chains. The corresponding charge densities can easily respond to a displacement of the neighboring ions by a variation of the charge accumulation between the ions. This can be viewed as arising from changes in hybridization of the $2p$ wave functions of the oxygen with the $5d$ and $4d$ wave functions of Ta and Nb, respectively. The strong response of the O^{2-} polarizability to the lattice displacements in normal modes causes the strong second-order Raman spectra in the oxidic perovskites. The same interpretation has been proposed for oxidic II-VI compounds with rocksalt structure like MgO and SrO.[29,30] The nonlinearities may also be the origin of the strong electro-optic properties[43] and the large hyper-Raman scattering cross sections of the oxidic perovskite type crystals.[44]

Our calculations have revealed a strong correlation between the shell eigenvectors of the O^{2-} ions and those of the B ions. We have found that an enhancement of the oxygen core-shell eigenvector yields an enhancement of the core-shell eigenvector of the B ions (in the directions of the O-B chains). In other words, it is possible to obtain softening of the ferroelectric mode by a variation of the core-shell coupling of the B ion. This observation reinforces the idea of dynamical hybridization along the O-B chains.

A last interesting point concerns the respective influences of the linear k_2^{O-B} and nonlinear k_4^{O-B} coupling parameters on the softening of the ferroelectric mode and on the transition temperature T_c. If the thermal average of the oxygen shell displacement in the B ion direction is approximated by a linear function (see Fig. 3):

$$\langle w_{O-B}^2 \rangle_T = a + bT \ , \tag{10}$$

the core-shell coupling constant along the O-B chain becomes a linear function of the temperature:

$$k_{O-B}(T) = k_2^{O-B} + (ak_4^{O-B} + bk_4^{O-B}T)/2 \ . \tag{11}$$

In Fig. 5, we present schematically these functions for different niobium concentrations. It is evident that the rate of the ferroelectric mode softening is substantially affected by the nonlinear parameter k_4^{O-B} which enters in the temperature dependent part. The phase transition temperature T_c is the temperature where the ferroelectric mode has a frequency equal to zero. Our calculations yield for $k_{O-B}(T)$ the values 351.0 for $KTaO_3$ and 343.7 for $KNbO_3$. The difference between these two values is due to the difference in mass of the B ions. Since the term $ak_4^{O-B}/2$ in the temperature-independent contribution to $k_{O-B}(T)$ is small compared to k_2^{O-B}, the increase of T_c with increasing niobium concentration is essentially due to the decrease of k_2^{O-B}. The temperature of the phase transition is obtained in Fig. 5 at the intersection of zero-frequency line with the function $k_{O-B}(T)$. In the case of $KNbO_3$, it is remarkable that the phase transition takes place at about 300 K which is near the transition temperature between the orthorhombic and rhombohedral phases. This is in agreement with the fact that an extrapolation of the ferroelectric mode frequency squared from the cubic phase yields a zero frequency near this last phase transition.[6]

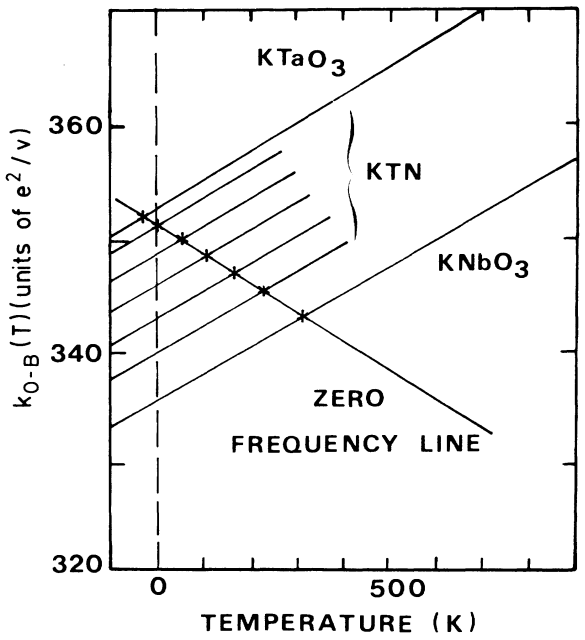

FIG. 5. Schematic representation of the respective influences of the linear k_2^{O-B} and nonlinear k_4^{O-B} coupling constants on the phase transition. The parameter k_4^{O-B} governs the rate of the mode softening given by the slope of $k_{O-B}(T)$. The temperature T_c is given by the intersection of the zero-frequency line with the $k_{O-B}(T)$ functions which are essentially determined by the linear coupling constant k_2^{O-B}.

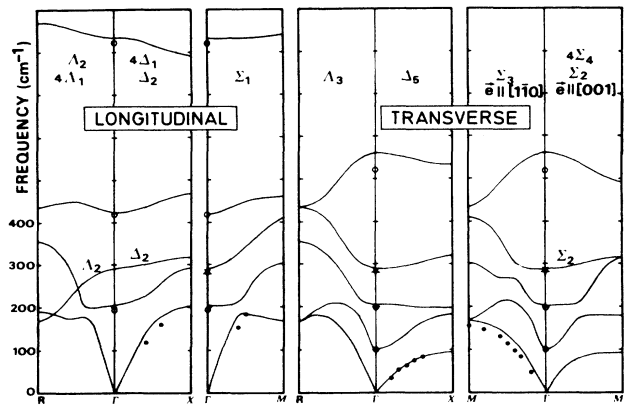

FIG. 6. Phonon dispersion curves calculated for $KNbO_3$ at 730 K and compared with experimental data obtained by neutron scattering (solid circles) (Ref. 45), ir spectroscopy (open circles) (Ref. 6), and Raman spectroscopy (stars) (Ref. 46).

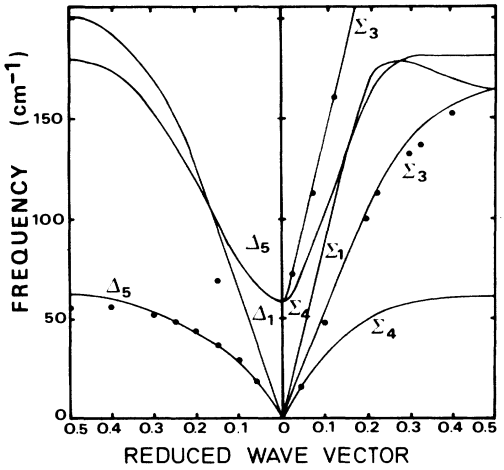

FIG. 7. Low-frequency phonon dispersion curves calculated for $KTa_{1-x}Nb_xO_3$ ($x=37\%$) and compared with neutron scattering data (Ref. 42).

C. Calculation of the dispersion curves

Until now our discussion was focused specially on the soft-mode behavior at the center of the Brillouin zone. Migoni *et al.*[41] have shown that the set of parameters used in our calculations reproduces the measured phonon dispersion curves of $KTaO_3$ in the three high-symmetry directions within experimental error. In order to provide additional evidence for the validity of the model, we calculated the whole set of dispersion curves of $KNbO_3$ in the cubic phase at a temperature of 730 K. The results are presented in Fig. 6 together with the neutron scattering data of Nunes *et al.*[45] and the ir reflectivity data of Fontana *et al.*[6] The star symbol indicates the frequency of the silent mode measured in $KNbO_3$ in the tetragonal phase.[46] This frequency remains unmodified when the tetragonal to cubic transition is crossed. Comparison shows good agreement between the calculations and the measurements.

Good agreement is also obtained for the low-frequency dispersion branches of KTN with $x=0.37$, which have been determined by Yelon *et al.*[42] The experimental points at 340 K of Yelon are compared with our calculations in Fig. 7. The strong coupling of the soft ferroelectric mode with the transverse acoustic branches of Δ_5 and Σ_4 symmetry is correctly reproduced within the framework of our calculation.

The phonon dispersion curves for various other compositions of KTN have been performed and compared with recent unpublished experimental data of the authors. The details will be discussed in a forthcoming paper.

IV. CONCLUSION

We have shown that the phonon dispersion of solid solutions $KTa_{1-x}Nb_xO_3$ can be described in the whole range of niobium concentration between 0% and 100% within the framework of a nonlinear shell model. This model has only two concentration-dependent parameters $k_2^{O\text{-}B}$ and $k_4^{O\text{-}B}$, which describe the linear and nonlinear oxygen polarizability. All other parameters are concentration independent. Our results indicate that not only the temperature dependence of the ferroelectric soft mode but also its dependence on the niobium concentration is exclusively governed by the oxygen polarizability and its variation with the niobium concentration due to hybridization of the oxygen p states with the transition metal d states.

Of course, our model cannot provide the phonon linewidth, which is governed by third-order anharmonic terms, as shown, for example, by Bruce and Cowley.[26] Since the damping of the ferroelectric mode increases with increasing niobium concentration, the influence of these terms will increase as well.

ACKNOWLEDGMENTS

We are grateful to Professor H. Bilz, Professor C. Carabatos, Dr. D. Rytz, and Dr. H. Vogt for helpful and stimulating discussions. One of us (G.E.K.) would like to thank the Max-Planck-Institut für Festkörperforschung (Stuttgart) for its hospitality.

[1]D. Rytz, Ph.D. thesis, Ecole Polytechnique Fédérale de Lausanne, 1983.
[2]U. T. Höchli, H. E. Weibel, and L. A. Boatner, Phys. Rev. Lett. 39, 1158 (1977).
[3]D. Rytz, U. T. Höchli, and H. Bilz, Phys. Rev. B 22, 359 (1980).
[4]A. W. Hewat, J. Phys. C 6, 2559 (1973).
[5]G. Shirane, H. Danner, A. Pavlovic, and R. Pepinsky, Phys. Rev. 93, 672 (1954).
[6]M. D. Fontana, G. Metrat, J. L. Servoin, and F. Gervais,

J. Phys. C **17**, 483 (1984).
[7]M. D. Fontana, G. Metrat, J. L. Servoin, and F. Gervais, Ferroelectrics **38**, 797 (1981).
[8]R. C. Miller and W. G. Spitzer, Phys. Rev. **129**, 94 (1963).
[9]C. H. Perry and T. F. McNelly, Phys. Rev. **154**, 456 (1967).
[10]C. H. Perry and N. E. Tornberg, Phys. Rev. **183**, 595 (1969).
[11]G. Shirane, R. Nathans, and V. J. Minkiewicz, Phys. Rev. **157**, 396 (1967).
[12]P. A. Fleury and J. M. Worlock, Phys. Rev. Lett. **18**, 665 (1967); Phys. Rev. **174**, 613 (1968).
[13]H. Vogt and H. Uwe, Phys. Rev. B **29**, 1030 (1984).
[14]R. Kind and K. A. Müller, Commun. Phys. **1**, 223 (1976).
[15]K. A. Müller and H. Burkhard, Phys. Rev. B **19**, 3593 (1979).
[16]G. E. Kugel, H. Vogt, W. Kress, and D. Rytz, Phys. Rev. B **30**, 985 (1984).
[17]T. Schneider, H. Beck, and E. Stoll, Phys. Rev. B **13**, 1123 (1976); R. Oppermann and H. Thomas, Z. Phys. B **22**, 387 (1975).
[18]D. Rytz, M. D. Fontana, J. L. Servoin, and F. Gervais, Phys. Rev. B **28**, 6041 (1983).
[19]S. K. Manlief and H. Y. Fan, Phys. Rev. B **5**, 4046 (1972).
[20]W. Cochran, Adv. Phys. **9**, 387 (1960); **10**, 401 (1961).
[21]R. A. Cowley, Adv. Phys. **29**, 1 (1980).
[22]J. C. Slater, Phys. Rev. **78**, 748 (1950).
[23]A. A. Maradudin and A. E. Fein, Phys. Rev. **128**, 2589 (1962). A. A. Maradudin and P. A. Flynn, *ibid* **129**, 2529 (1963); Ann. Phys. **22**, 223 (1963).
[24]R. A. Cowley, Adv. Phys. **12**, 421 (1963); Philos. Mag. **11**, 673 (1964); Phys. Rev. B **13**, 4877 (1976); Phys. Rev. Lett. **36**, 744 (1976).
[25]E. Pytte and J. Feder, Phys. Rev. **187**, 1077 (1969); E. Pytte, Phys. Rev. B **5**, 3758 (1972).
[26]A. D. Bruce and R. A. Cowley, J. Phys. C **6**, 2422 (1973).
[27]N. Gillis, Phys. Rev. Lett. **22**, 1251 (1969); B. D. Silverman and R. I. Joseph, Phys. Rev. **129**, 2062 (1963); **133**, A207 (1964).
[28]M. Buchanan, R. Haberkorn, and H. Bilz, J. Phys. C **7**, 439 (1974).
[29]R. Migoni, K. H. Rieder, K. Fischer, and H. Bilz, Ferroelectrics **13**, 377 (1976).
[30]R. Migoni, H. Bilz, and D. Bäuerle, Phys. Rev. Lett. **37**, 1155 (1976).
[31]R Migoni, H. Bilz, and D. Bäuerle, in *Lattice Dynamics,* edited by M. Balkanski (Flammarion, Paris, 1978), p. 650.
[32]H. Bilz, A. Bussmann, G. Benedek, H. Büttner, and D. Strauch, Ferroelectrics, **25**, 335 (1980).
[33]A. Bussmann-Holder, G. Benedek, H. Bilz, and B. Mokross, J. Phys. (Paris) Colloq. **42**, C6-409 (1981).
[34]A. Bussmann-Holder, H. Bilz, D. Bäuerle, and D. Wagner, Z. Phys. B **41**, 353 (1981).
[35]M. Balkanski, M. K. Teng, M. Massot, and H. Bilz, Ferroelectrics **26**, 737 (1980).
[36]A. Bussmann-Holder, H. Bilz, and W. Kress, J. Phys. Soc. Jpn. **49**, Suppl. A, 737 (1980).
[37]A. Bussmann-Holder, H. Büttner, and H. Bilz, Ferroelectrics **35**, 273 (1981).
[38]R. A. Cowley, Phys. Rev. **134**, A981 (1964).
[39]W. Stirling, J. Phys. C **5**, 2711 (1972).
[40]M. Fontana, G. Kugel, and C. Carabatos, J. Phys. (Paris) **42**, 66 (1981).
[41]R. L. Migoni, R. Currat, C. H. Perry, H. Buhay, W. G. Stirling, and J. D. Axe (private communication).
[42]W. B. Yelon, W. Cochran, G. Shirane, and A. Linz, Ferroelectrics **2**, 261 (1971).
[43]P. Gunter, Ferroelectrics **24**, 35 (1980).
[44]H. Vogt and G. Rossbroich, Phys. Rev. B **24**, 3086 (1981).
[45]A. C. Nunes, J. D. Axe, and G. Shirane, Ferroelectrics **2**, 231 (1971).
[46]M. D. Fontana, G. E. Kugel, G. Metrat, and C. Carabatos, Phys. Status Solidi B **103**, 211 (1981).